

## **THERMAL ANALYSIS OF SOLID-SOLID INTERACTIONS IN BINARY MIXTURES OF ALKYL CYCLOHEXANES USING DSC**

*P. H. Young*<sup>1</sup>, *D. Dollimore*<sup>2</sup> and *C. A. Schall*<sup>1\*</sup>

<sup>1</sup>University of Toledo, Department of Chemical and Environmental Engineering  
2801 W. Bancroft, Toledo, OH 43606

<sup>2</sup>University of Toledo, Department of Chemistry, 2801 W. Bancroft, Toledo, OH 43606 USA

(Received April 17, 2000)

### **Abstract**

Differential scanning calorimetry (DSC) was used to construct phase diagrams of binary mixtures of alkylcyclohexanes and to characterize metastable phases formed in the binary mixtures. The experimentally measured liquidus curves were compared to the liquidus curves calculated using ideal solution theory. The measured phase diagrams of pentadecylcyclohexane/nonadecylcyclohexane and octadecylcyclohexane/nonadecylcyclohexane binary mixtures are consistent with theoretical phase diagrams constructed based on the assumption that these mixtures form eutectic systems. It was also observed that a metastable phase formed in some binary mixtures of pentadecylcyclohexane/nonadecylcyclohexane under fast cooling conditions. It is hypothesized that this metastable phase recrystallizes into the eutectic phase upon heating.

**Keywords:** alkylcyclohexanes, binary phase diagrams, DSC, metastable solutions

### **Introduction**

Hydrocarbon mixtures have been studied extensively in order to predict solution behavior and to model the precipitation of waxes from hydrocarbon fuels and crude oil mixtures. The majority of the studies have focused on normal alkanes while little is known about the solution behavior of other components of crude oils and fuels. It is known that crude oils contain a complex mixture of high molecular mass compounds including normal and isoalkanes, naphthenes and naphthalenes [1]. In particular, the solution behavior of alkylcyclohexane mixtures is largely unstudied.

The distinction of whether mixture components form solid solutions or eutectic solids, is important in predicting the solubility of solids in solution [2]. In binary solutions it is easily shown that components forming eutectic solids are predicted to have a higher

\* Author to whom all correspondence should be addressed.

solubility than components that form solid solutions. Additionally, the physical characteristics of solid precipitates are strongly influenced by the solid structure [3].

In our studies, differential scanning calorimetry (DSC) was used to study the solid-solid miscibility of alkylcyclohexane mixtures by constructing the phase diagrams of binary mixtures of pentadecylcyclohexane/nonadecylcyclohexane ( $CC_{21}/CC_{25}$ ) and octadecylcyclohexane/nonadecylcyclohexane ( $CC_{24}/CC_{25}$ ). DSC was also used to characterize phase transitions observed in some of these mixtures. The experimentally measured liquidus curves were compared to the liquidus curves constructed using ideal solution theory.

DSC is a useful technique in characterizing the phase behavior of mixtures. DSC can provide information on the number of phase transitions, the enthalpies of phase transitions and transition temperatures. DSC results, combined with the application of thermodynamics, can be used to distinguish whether the binary mixtures of alkylcyclohexanes form solid solutions or eutectic systems [4].

In previous studies of normal alkanes, mixtures of  $n$ -alkanes have been found to form metastable solid solutions when the chain length differences between the mixture components are small [3, 5, 6]. Microphase separation and subsequent demixing have been reported for rapidly quenched mixtures of  $n$ -alkanes [7]. This demixing takes place within a highly crystalline solid. In our studies with alkylcyclohexane mixtures, the formation of a metastable solid phase in some mixtures of pentadecylcyclohexane/nonadecylcyclohexane was observed. The composition of this metastable phase was determined using mass balances deduced from DSC traces.

#### *The phase diagrams of simple eutectic systems and solid solutions*

Simple eutectic systems yield pure crystalline solids of each component when cooled. Figure 1A illustrates the relationship between composition and solidification temperatures for all A/B mixtures in a simple binary eutectic system. When the mixtures are partially solidified at temperatures below  $T_A$  or  $T_B$ , the melting points of A and B respectively, pure crystalline solids of A and B are in contact with the molten mixtures. It can be seen that there are two branches to the melting curve, intersecting at point E, the lowest temperature at which a molten A/B mixture can exist. This point is called the eutectic (easily melt; from  $\epsilon\nu$  well and  $\tau\eta\kappa\epsilon\iota\nu$  to melt) [4].

The shape of the  $T_AET_B$  curve can be calculated by the application of thermodynamics. An equation relating the mole fraction,  $x$ , of A soluble in B at a temperature  $T$  can be developed assuming: A and B form ideal solutions, that changes in heat capacity between solid and liquid phases are negligible and the melting point  $T_A$  can be substituted for the triple point. The resulting equation is:

$$\ln x = \frac{\Delta H_A}{R} \left( \frac{1}{T_A} - \frac{1}{T} \right) \quad (1)$$

where  $\Delta H_A$  is the molar latent heat of fusion of component A (assumed to be temperature independent) at its melting point,  $T_A$ , and  $R$  is the gas constant. A similar equation is valid for component B dissolved in solvent A. It follows that if the heats of fu-

sion and melting point temperatures for both components are known, then the eutectic temperature and composition may be calculated as the intersection between the two branches of the melting curve as seen in Fig. 1A.

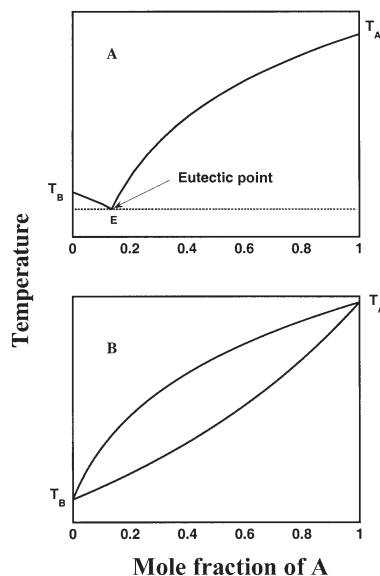


**Fig. 1** The phase diagram of a simple eutectic system consists of two branches of melting curves which intersect at the eutectic point. The dashed line represents the eutectic temperature. The DSC curves will consist of at least two liquid-solid transitions for the pure component and eutectic mixture (A). The liquidus curve of the solid solution phase diagram does not have two branches as do the liquidus curves of the eutectic system. Additionally, solid precipitate consists of a single phase. The DSC curves of binary mixtures that form solid solutions are expected to contain a single liquid-solid phase transition peak whose end point is located on the liquidus curve (B)

Cooling a mixture whose composition lies to the left of the eutectic in the phase diagram will give a solid consisting of pure B while cooling a mixture whose composition lies to the right will give a solid consisting of pure A. Conventionally, mixtures are named according to whether their composition lies to the left or to the right of the eutectic; the former are called hypoeutectic and the latter are called hypereutectic.

The phase diagram of a binary mixture of a solid solution is shown in Fig. 1B. The phase diagram of solid solutions of binary mixtures can be predicted based on the same assumptions used to develop Eq. (1) except that the solid phase now consists of a solid solution instead of a pure solid phase. The melting curves of the phase diagrams are calculated using the following thermodynamic and stoichiometric relationships:

$$\ln \frac{x_A}{x_A^S} = \frac{\Delta S_A}{R} - \frac{\Delta H_A}{RT} \quad (2)$$

$$\ln \frac{x_B}{x_B^S} = \frac{\Delta S_B}{R} - \frac{\Delta H_B}{RT} \quad (3)$$

$$x_B = 1 - x_A \quad (4)$$

$$x_B^S = 1 - x_A^S \quad (5)$$

where  $x_A$  and  $x_B$  are mole fractions of component A and B in the molten phase of the mixture and  $x_A^S$  and  $x_B^S$  are mole fraction of A and B in the solid phase of the mixture. The four variables  $x_A$ ,  $x_B$ ,  $x_A^S$  and  $x_B^S$  can be solved for by simultaneous solution of Eqs (2)–(5).

The phase diagram of a mixture of two components can be constructed using DSC to measure phase transition temperatures for solutions of varying composition. The experimental phase diagram is then compared to the theoretical phase diagram constructed using Eqs (1) to (5).

## Experimental

### Instrumentation

The calorimetry experiments were performed on a Calorimetry Sciences Corporation, CSC, 4100 multi-cell differential scanning calorimeter. The CSC 4100 is a heat-flux DSC equipped with three Hasteloy sample cells and a reference cell, each with a capacity of 1 ml. The sensitivity of the DSC detectors (piezoelectric devices), as specified by the manufacturer, is approximately  $40 \mu\text{J } ^\circ\text{C}^{-1}$ . The temperature range of the DSC is  $-20$  to  $200^\circ\text{C}$  with scan rates (heating or cooling) of  $0.1$  to  $2^\circ\text{C min}^{-1}$ . During the scanning operation, argon was purged through the DSC chamber at  $4.0 \text{ ml min}^{-1}$ .

The CSC DSC was used to construct the phase diagram of  $\text{CC}_{21}/\text{CC}_{25}$  binary mixtures. The mixtures were heated to  $75^\circ\text{C}$  at  $2.0^\circ\text{C min}^{-1}$ , held for 5 min, cooled to  $-20^\circ\text{C}$  at  $2.0^\circ\text{C min}^{-1}$ , held for 5 min, and then heated  $75^\circ\text{C}$  at  $0.1^\circ\text{C min}^{-1}$ . During the scanning operation, argon was purged through the DSC chamber at  $4.0 \text{ ml min}^{-1}$ .

A Perkin Elmer Pyris I DSC was also used in our studies because of its greater temperature range and faster scanning rates. The Pyris I DSC has a temperature range from  $-170$  to  $600^\circ\text{C}$  with heating rates between  $5$  to  $40^\circ\text{C min}^{-1}$ . The Pyris I DSC is equipped with a CryoFill® cooling system which uses liquid nitrogen to cool the samples down to  $-170^\circ\text{C}$  in sub-ambient experiments. The Pyris I DSC was used to construct a phase diagram of  $\text{CC}_{24}/\text{CC}_{25}$  binary mixtures and to confirm the results of the CSC DSC studies when an extended temperature range was required. Helium was used as a purge gas in the Pyris I DSC.

### Materials

Pentadecylcyclohexane,  $\text{CC}_{21}$  (Lot# FCZ01), octadecylcyclohexane,  $\text{CC}_{24}$  (Lot# FCU01), and nonadecylcyclohexane,  $\text{CC}_{25}$  (Lot# FII01), were obtained from TCI America with purities verified by gas chromatographic (GC) analysis. A Shimadzu GC equipped with a Restek RTX-1® 30 m by 0.53 mm ID capillary column and a

flame ionization detector was used for the chromatographic method. The purities of penta-, octa-, and nona-decylcyclohexane were determined to be 99.7, 98.8, and 99.1% respectively. Hexadecane (Lot# 13412PR), triacontane (Lot# JN04722HN), (purity $\geq$ 99%) and cyclohexane (Lot# JU20979LS) (purity $\geq$ 99.9%) were used for temperature and enthalpy calibration and were purchased from Sigma Aldrich.

#### *Preparation of the samples*

For experiments conducted on the CSC 4100, samples of the binary mixtures of alkylcyclohexane were prepared by mass directly in the Hastelloy cells provided by CSC. For experiments that were conducted in the Perkin Elmer Pyris I DSC, samples were first weighed into 1.5 ml glass vials and then melted to mix the sample, cooled, and then a portion of the solid sample was transferred into aluminum sample pans and crimp-sealed.

#### *Enthalpy of melting measurement*

The melting and crystallization heat signal measured by DSC varies with heating and cooling rates. In order to quantify the amount of a sample undergoing a phase transition from the DSC traces of  $CC_{21}/CC_{25}$  mixtures, the enthalpies of phase transitions were measured for pure  $CC_{25}$ , pure  $CC_{21}$ , and the eutectic mixture (mole fraction of  $CC_{25}$  equal to 0.137) at a heating rate of 0.1 and a cooling rate of  $2.0^\circ\text{C min}^{-1}$  using the CSC DSC. The measured heat signals of the CSC DSC were calibrated using the melting enthalpy of cyclohexane [8]. At  $0.1^\circ\text{C min}^{-1}$  heating rate, the integrated heat signals for  $CC_{25}$ ,  $CC_{21}$ , and eutectic primary phase transitions were determined to be 222, 198 and  $176 \text{ J g}^{-1}$  (77.8, 58.3,  $53.2 \text{ kJ mol}^{-1}$ ) respectively. Two overlapping exothermic peaks were visible on cooling traces of  $CC_{25}$ , but only a single endothermic peak was detectable on sample melting (data not shown). At a  $2.0^\circ\text{C min}^{-1}$  cooling rate, the heat signals for  $CC_{25}$ ,  $CC_{21}$ , and eutectic phase were 182, 166, and  $122 \text{ J g}^{-1}$  ( $63.8, 48.9, 36.9 \text{ kJ mol}^{-1}$ ) respectively.

## **Results and discussion**

For pure samples, the onset of the endothermic melting peak in the DSC heating traces provides the melting point temperatures of samples. For mixtures, the melting points of the separate phases in the mixtures are best determined from the extrapolated end points of the endothermic melting peaks. Details on determining the onset and the extrapolated end points of endothermic melting peaks are given in a text by Hohne *et al.* [9]. For binary mixtures of simple eutectic systems, two endothermic melting peaks are present in a DSC trace (Fig. 2). These can be assigned to the melting of the eutectic and the pure component phase. The extrapolated end point of the second endothermic peak corresponds closely to the temperature calculated using Eq. (1).

For  $CC_{21}/CC_{25}$  binary mixtures, the experimentally determined solid phase diagram, Fig. 3A, was constructed using DSC traces obtained from the CSC DSC. The

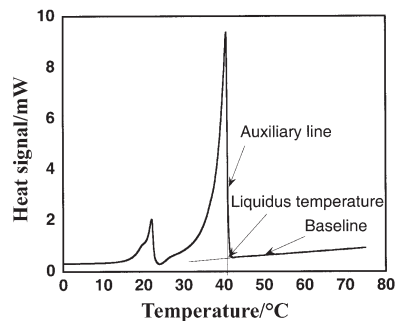


**Fig. 2** The DSC curve shown here is from a heating scan of a hypereutectic  $CC_{21}/CC_{25}$  mixture (0.805 mole fraction of  $CC_{25}$ ). There are two endothermic melting peaks in the figure. The first peak near  $20^{\circ}\text{C}$  is attributed to melting of the eutectic phase and the second peak near  $40^{\circ}\text{C}$  is attributed to the melting of pure  $CC_{25}$ . The auxiliary line is the linear extrapolation of the descending section of the peak. The baseline is the linear interpolation of the signals after the peak. The liquidus temperature is taken as the intersection between the auxiliary line and the extrapolated baseline

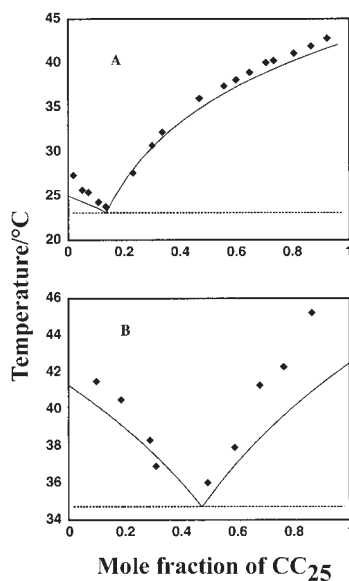


**Fig. 3** Both the  $CC_{21}/CC_{25}$  3A and  $CC_{24}/CC_{25}$  3B phase diagrams indicate the formation of eutectic solids in mixtures of alkylcyclohexanes. The solid diamonds represent the liquidus temperature of the mixtures determined from DSC curves. The solid lines represent the liquidus curves predicted by Eq. (1). Experimental data in (A) were obtained using curves from the CSC DSC with a heating rate of  $0.1^{\circ}\text{C min}^{-1}$  and data in (B) were obtained using thermograms from the PE Pyris I DSC with a heating rate of  $5^{\circ}\text{C min}^{-1}$ . The larger deviation of experimental data points in 3B may be a result of the faster heating rate. Both plots have two distinct branches in their melting curves that identify them as eutectic systems

phase diagram indicates that  $CC_{21}/CC_{25}$  binary mixtures form a eutectic system. Deviation of the experimental data from the predicted solid-liquidus curve using Eq. (1) may be due in part to non-idealities of liquid solutions or significant heat capacity differences between solid and liquid phases.

For  $CC_{24}/CC_{25}$  binary mixtures, the experimentally determined solid phase diagram, Fig. 3B, was constructed using DSC traces obtained from the Pyris I DSC. Formation of eutectic solids is also indicated in the  $CC_{24}/CC_{25}$  phase diagram. The larger deviation of experimental data points from the predicted values seen in Fig. 3B compared to data shown in Fig. 3A may be a result of the faster heating rate used in the Pyris I DSC.

The composition of the eutectic phase of the binary  $CC_{21}/CC_{25}$  mixtures can be obtained either by solving Eq. (1) for both components simultaneously or experimentally by constructing a Tammann plot (Fig. 4) [4]. The eutectic phase composition of  $CC_{21}/CC_{25}$  binary mixtures as calculated from Eq. (1) was 0.137 mole fraction of  $CC_{25}$ . The eutectic phase composition obtained by the Tammann plot was 0.143 mole fraction of  $CC_{25}$ , in good agreement with the calculated composition using Eq. (1).

For simple eutectic systems, two endothermic melting peaks are expected in the DSC traces upon heating the hypoeutectic or hypereutectic samples. A single endothermic melting peak is expected in the DSC traces when heating the samples of eutectic composition. As can be seen in the DSC trace in Fig. 5A, a single endothermic peak is observed in the sample of eutectic composition but additional peaks are observed in samples with hypoeutectic (Fig. 5B) or hypereutectic (Fig. 5C) compositions. The small endothermic peak observed at  $8^{\circ}\text{C}$  and  $-1^{\circ}\text{C}$  in hypoeutectic (Fig. 5B), and hypereutectic (Fig. 5C) mixtures, respectively, are similar to the small peaks assigned to changes in interlamellar packing in studies conducted on normal alkanes by Takamizawa *et al.* [10]. The two endothermic peaks following this small

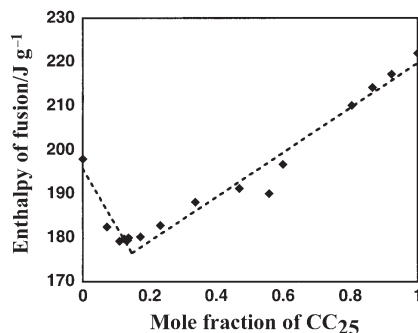


**Fig. 4** The Tammann plot for  $CC_{21}/CC_{25}$  mixtures is constructed by plotting the enthalpy of fusion vs. the sample composition, solid diamonds. The enthalpy of fusion is obtained by integrating the areas of both the eutectic peak and the pure component peak and dividing the integrated heat signal by the total sample mass. The Tammann plot provides an experimental means of determining the composition of the eutectic phase. The eutectic composition is determined to be 0.143 mole fraction of  $CC_{25}$  from the data above compared to a calculated value of 0.137

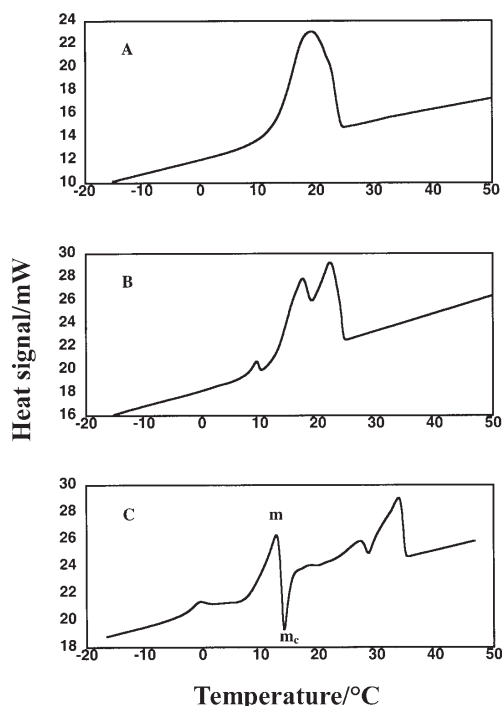


**Fig. 5** Heating curves of 5A eutectic, 0.137 mole fraction of  $CC_{25}$ , 5B hypo-eutectic, 0.0507 mole fraction of  $CC_{25}$  and 5C hyper-eutectic mixtures, 0.451 mole fraction of  $CC_{25}$  in  $CC_{25}/CC_{21}$  mixtures obtained on a PE Pyris I DSC at a  $5^{\circ}\text{C min}^{-1}$  heating rate. In the hyper-eutectic mixture a large endothermic 'melting' peak,  $m$ , followed by an exothermic 'crystallization' peak,  $mc$  is observed

peak in the hypo-eutectic mixture (Fig. 5B) can be attributed to melting of the eutectic phase followed by melting of pure  $CC_{21}$  phase.

A large endothermic peak immediately followed by a large exothermic peak is present in the DSC heating trace of the hyper-eutectic mixture (Fig. 5C) prior to the endothermic melting peak of the eutectic phase. These transitions were only observed when hyper-eutectic mixtures of  $CC_{21}/CC_{25}$  were cooled quickly and are attributed to melting and re-crystallization of a metastable phase. The melting point of this phase was below that of the eutectic, pure  $CC_{21}$ , and  $CC_{25}$  phases. This metastable phase was found to form only in hyper-eutectic mixtures of  $CC_{21}/CC_{25}$  with  $CC_{25}$  mole fractions of less than 0.800 and was not observed when samples were slowly cooled (less than  $2^{\circ}\text{C min}^{-1}$ ). The metastable phase melting and crystallization peaks could not be separated using the Pyris I DSC. The two endothermic peaks following the exotherm (Fig. 5C) are attributed to melting of the eutectic solid followed by melting of pure  $CC_{25}$ .



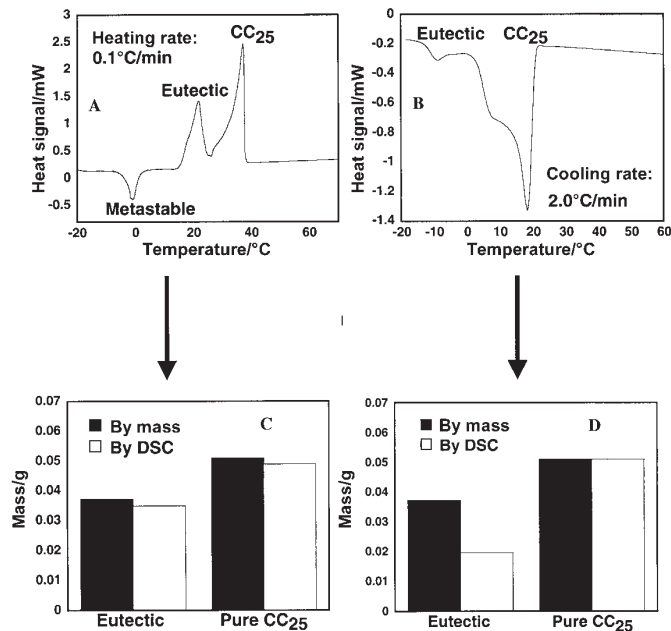


**Fig. 6** Heating and cooling traces of a hypereutectic mixture of CC<sub>21</sub>/CC<sub>25</sub> (mole fraction of CC<sub>25</sub> of 0.604) using the CSC DSC. (A) On the DSC curve we can see one crystallization peak (metastable phase) and two endothermic melting peaks (eutectic phase and pure CC<sub>25</sub> phase). Below the DSC curve is the bar graph (C) comparing the masses of the eutectic phase and pure CC<sub>25</sub> phase calculated by sample composition and their actual masses (black blocks) and masses calculated from the DSC curve (white blocks), assuming that CC<sub>25</sub> completely crystallizes. (B) The cooling curve of the same sample, indicates that initially not all of the mass of the sample has crystallized into the eutectic phase and the pure CC<sub>25</sub> phase. The total measured exothermic signal corresponds to a sample mass of 0.0704 g, which was 20% less than the weighed mass of 0.0881 g as illustrated in (D).

A binary mixture of CC<sub>21</sub>/CC<sub>25</sub> with a mole fraction of CC<sub>25</sub> of 0.604 (0.0568 g of CC<sub>25</sub> and 0.0313 g of CC<sub>21</sub>) was prepared and both heating and cooling DSC traces were obtained using the CSC DSC. The heating trace obtained at a slow heating rate, 0.1°C min<sup>-1</sup> (Fig. 6A), consists of one exothermic crystallization peak and two endothermic melting peaks. The third endothermic peak attributed to melting of the metastable solid (Fig. 5C) was not observable in the CSC DSC curves due to the limited temperature range of this DSC. On cooling of the sample, three exothermic peaks are observed (Fig. 6B). The overlapping peaks observed at higher temperature are consistent with overlapping peaks observed in cooling curves of pure CC<sub>25</sub> indicating a possible solid-solid transition. The exothermic peak at the lower temperature is assigned to solidification of the eutectic phase (Fig. 6A).

It is hypothesized that the metastable solid phase has the same composition as the eutectic phase. It is further hypothesized that the pure  $CC_{25}$  phase has completely crystallized in hypereutectic mixtures. Using enthalpies of melting obtained at the appropriate heating and cooling rate (see Materials and Methods) it is possible to verify this hypothesis using mass balance calculations.

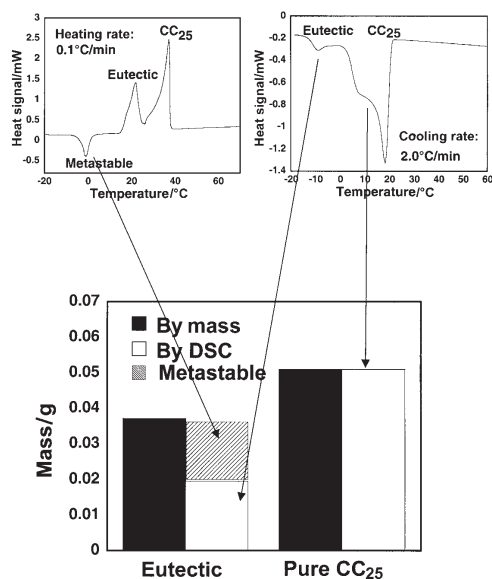


**Fig. 7** Analysis of both the heating and cooling curve of the  $CC_{21}/CC_{25}$  hypereutectic mixture. When it was assumed that the composition of the metastable phase was identical to the eutectic phase, the masses of the metastable phase, the eutectic phase, and the pure  $CC_{25}$  phase summed up to 98% of the total mass and thus closing the mass balance

The DSC traces of a binary mixture of  $CC_{21}/CC_{25}$  with a mole fraction of  $CC_{25}$  of 0.604 were analyzed (Figs 6 and 7). The heating trace obtained at a heating rate of  $0.1^\circ\text{C min}^{-1}$  (Fig. 6A), consists of one exothermic crystallization peak and two endothermic melting peaks. Figures 6A and 6C illustrate how the two endothermic peaks sum up to the total mass (within 6%) weighed into the sample cell when the endothermic peaks were assumed to be the eutectic melting peak and the pure  $CC_{25}$  melting peak. This means that the metastable phase re-crystallized into either the eutectic phase or the pure  $CC_{25}$  phase.

Analysis of the endothermic peaks in the cooling traces of the sample in Fig. 6B shows that the mass of solid that has crystallized as pure component and eutectic was significantly less than expected (Fig. 6D and 7A). The total measured exothermic signal corresponds to a sample mass of 0.0704 g, which was 20% less than the weighed mass of 0.0881 g. When one makes the assumption that the pure  $CC_{25}$  phase has completely crystallized and the missing mass is due to the incomplete crystallization of eutectic phase, one can then determine the amount of eutectic phase that has crystal-

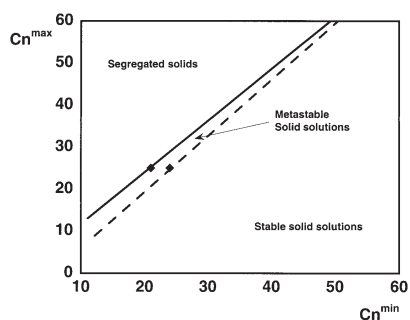


**Fig. 8** Region of metastable solid solutions. The figure shows the chain lengths of the long and short components of *n*-alkane mixtures for the formation of a stable solid solutions according to Dorset [3], dashed line and Matheson *et al.* [11], solid line. The horizontal axis represents the carbon number of the shorter component and the vertical axis represents the carbon number of the longer component. A binary mixture whose composition is located to the left of the solid line forms eutectic mixtures and a binary mixture whose composition is located to the right of the dashed line forms stable solid solutions. Mixtures located between these two lines have been found to form metastable solutions. The binary mixture of  $CC_{21}/CC_{25}$  and  $CC_{24}/CC_{25}$  (diamonds) can form metastable solid solutions if we assume that alkylcyclohexanes behave similarly to the normal alkanes

lized by subtracting the calculated  $CC_{25}$  signal from the experimentally measured exothermic signals (Figs 6 and 7).

Even though the CSC DSC did not record the crystallization of the metastable phase on the cooling trace, due to the instrument temperature range limitations ( $-20$  to  $200^{\circ}\text{C}$ ), the PE trace (Fig. 5) recorded the apparent melting of the metastable phase immediately followed by an apparent recrystallization. The CSC DSC was able to record the recrystallization of the metastable phase after melting. It was assumed that  $CC_{25}$  completely crystallized, the eutectic phase incompletely crystallized, and the metastable phase recrystallizes into the eutectic phase on heating. The resulting mass of the metastable phase calculated from the recrystallization peak produced on heating matches within 2% of the missing mass from the cooling curve (Fig. 7) of the  $CC_{21}/CC_{25}$  mixture, thus closing the mass balance.

## Conclusions

In order to appropriately model the solubility of complex mixtures of closely related solutes, it is important to know whether these solutes form solid solutions or eutectic systems. In the present investigation, it was found that the alkylcyclohexane mixtures formed eutectic systems for binary mixtures of pentadecylcyclohexane/nonadecylcyclohexane ( $CC_{21}/CC_{25}$ ) and octadecylcyclohexane/nonadecylcyclohexane ( $CC_{24}/CC_{25}$ ). In binary mixtures of *n*-alkanes, stable solid solutions generally form when the chain length differences between the components are less than four carbons [3, 5, 6]. However, this behavior exhibits a chain length dependency. As the *n*-alkane chain length of the shorter

component in binary mixtures increases, stable solid solutions can form with chain length differences of an increasing number of carbon atoms. On the other hand, as the chain length of the shorter component decreases, stable solid solutions can only form with decreasing chain length differences between the components [3]. Dorset [3] pointed out that an earlier study by Matheson *et al.* [11] indicated that the maximum chain length difference between the components of normal alkanes for formation of stable solid solutions was  $(0.224Cn^{\text{min}}-0.441)$  with  $Cn^{\text{min}}$  being the carbon number of the shorter component. Dorset, however, pointed out that further experiments indicated that some of the normal alkane mixtures that were formerly thought to be stable solid solutions were actually metastable because the mixtures fractionated after a period of either a few days or a few months. Dorset therefore reformulated the equation for predicting the maximum chain length difference between the components of stable solid solutions to be  $(0.33Cn^{\text{min}}-7.22)$ . It is therefore expected that *n*-alkane mixtures with chain length differences between  $(0.224Cn^{\text{min}}-0.441)$  and  $(0.33Cn^{\text{min}}-7.22)$  likely form metastable solid solutions as illustrated in Fig. 8. A normal alkane with a chain length of 21 is expected to form metastable solid solutions with normal alkanes with chain lengths up to 25; greater differences than this produce segregated solids. In the present investigation, mixtures of  $CC_{21}/CC_{25}$  appear to form a metastable solid solution in quench-cooled samples. This metastable solid solution apparently then re-crystallized into the eutectic phase. In binary mixtures of  $CC_{21}$  and  $CC_{25}$ , the formation of the metastable phase was observed when the concentration of the heavy component was greater than the eutectic but with a mole fraction of  $CC_{25}$  less than 0.80. The composition of this metastable phase is hypothesized to be that of the eutectic and may consist of a reordering of this phase upon sample heating similar to demixing of ordered solid solutions seen in quenched mixtures of *n*-alkanes [7]. Future work will include characterization of the metastable phase transition in alkylcyclohexane mixtures using X-ray powder diffraction or infrared spectroscopy.

Surprisingly, a metastable phase was not observed in mixtures of  $CC_{24}/CC_{25}$ . This could be due to differences in sample preparation from  $CC_{21}/CC_{25}$  mixtures. Additional experiments with quench-cooled mixtures of  $CC_{24}/CC_{25}$  are necessary to ascertain if these mixtures form metastable solutions.

\* \* \*

This work was supported through a DuPont-Conoco Young Professor Grant (CS) and an ACS-PRF grant 34437-AC9.

## References

- 1 A. Hood, R. J. Clerc and M. J. O'Neal, *J. Inst. Petroleum*, 45 (1959) 168.
- 2 J. M. Prausnitz, R. N. Lichtenthaler and E. G. Azevedo, *Molecular Thermodynamics of Fluid-Phase Equilibria.*, Prentice Hall PTR, Upper Saddle River 1999.
- 3 D. L. Dorset, *Macromolecules*, 23 (1990) 623.
- 4 G. Sloan and A. R. McGhie, *Techniques of Melt Crystallization*, John Wiley & Sons, Inc., New York 1988.
- 5 D. Clavell-Grunbaum, H. L. Strauss and R. G. Snyder, *J. Phys. Chem. B*, 101 (1997) 335.

- 6 B. K. Annis, J. D. Londono, G. D. Wignall and R. G. Snyder, *J. Phys. Chem.*, 100 (1996) 1725.
- 7 R. G. Snyder, M. C. Goh and V. J. P. Srivatsavoy, *J. Phys. Chem.*, 96 (1992) 10008.
- 8 J. G. Aston, G. J. Szasa and H. L. Fink, *J. Am. Chem. Soc.*, 65 (1943) 1135.
- 9 G. W. H. Hohne, W. Hemminger and H. J. Flammersheim, *Differential Scanning Calorimetry. An Introduction for Practitioners*, Springer-Verlag, New York, New York 1996.
- 10 K. Takamizawa, Y. Ogawa and T. Oyama, *Polymer Journal*, 14 (1982) 441.
- 11 R. R. Matheson, Jr. and P. Smith, *Polymer*, 26 (1985) 288.